Journal of Research and Applications in Mechanical Engineering
ISSN: 2229-2152 (Print); 2697-424x (Online)
(2024) Vol. 12, No. 1, Paper No. JRAME-24-12-003
[DOI: 10.14456/jrame.2024.3]

Research Article

Design and Analysis of Double Element Airfoil Using RANS

J. Chaiyanupong*
C. Khajorntraidet
Division of Mechanical and Automotive Engineering Technology, Faculty of Engineering and Technology, King Mongkut's University of Technology North Bangkok, Rayong campus, Rayong 21120, Thailand

Received 20 January 2023
Revised 29 May 2023
Accepted 12 June 2023

Abstract:
This paper aims to design the double-element airfoil for application on the front wing of a student formula car by using CFD (computational fluid dynamics) with the Reynolds Averaged Navia-Stokes (RANS) model. The design method is done by simulating the flow on a single-element airfoil to determine the separation point of fluid on the airfoil surface. The point is then used to divide the airfoil into the double-element airfoil, followed by analysis to find the right angle to achieve maximum downforce. The simulation results indicated that the angle of attack of 3° and the second element wing angle of 30° give the maximum Cl of 4.837, which can create downforce on the front wing of 884.3 N. It can be concluded that the designed double-element airfoil provides better downforce values than a single-element airfoil.

Keywords: *CFD, Front wing, Aerodynamics, Double element airfoil, Downforce*

1. Introduction

Formula One is a competition that has given rise to modern technology in the automotive industry. In the past, races focused on speeding cars as high as possible. However, as the competition develops further, racing cars have increased speed efficiently and have more power. Downforce under high speeds is, therefore, necessary to increase driving stability and reduce understeer. [1]. Modern racing cars achieve a literal acceleration of about 4g, which is 4 times the weight of the car. In theory, it can cause a car to overturn. The trend in improving aerodynamic and cornering speeds over the past 50 years has been the use of aerodynamic downforce [2]. The front wing of the race car is one of the most aerodynamic components. Researchers, therefore, focus on front-wing studies to improve the downforce.

The double-element wing was first introduced by McLaren in 1984, and the regulation allows the angle of attack of the second element to be adjusted so that the load enhanced on the front wing can be varied to balance the car according to various conditions [1]. The double-element front wing of a race car was experimentally studied by Jasinski and Selig [3]. The chosen airfoil was fitted with an endplate and had varying ground clearance of double element wings. The result shows that the downforce increased as the Reynolds number increased.

In 1997, Ranzenbach et al. [4] studied the double element of the NACA 632-215 Mod B airfoil experimentally and numerically. The result shows that the downforce changes as a function of the ground clearance. An experimental study of the aerodynamics of double element wings by Zhang and Zerihan [5] was conducted to investigate the ground effect and optimum-second element wing angle.

* Corresponding author: J. Chaiyanupong
E-mail address: Jaruwan.t@eat.kmutnb.ac.th

Nowadays, CFDs have evolved to the next level. It is a powerful tool that saves both time and resources in computing. As is known, the characteristics of the flow through the wing are usually complex. The simulation needs accurate predictions of aeronautics flow with strong adverse pressure gradients and separation. The CFD model that succeeds in computing this flow must be able to capture the proper behavior of turbulent boundary layers up to separation. CFD with Reynolds Averaged Navier-Stokes Simulation (RANS) is the method that is designed to solve the turbulent flow.

The efficiency of double-element airfoils in increasing downforce has been demonstrated according to the above-mentioned research, coupled with the efficiency of predicting the flow field of CFD Nowadays, CFDs can be used to help design a better double-element airfoil.

This paper aims to use CFD with the RANS model to design double-element airfoils for application on a student formula car front wing. Beginning with a 2-dimensional flow simulation through a single-element airfoil using three turbulent models. The results were then compared with the experimental results to find the most accurate turbulent model, including the separation point. The separation onset archived determines the split distance of the double-element airfoil. Finally, the aerodynamic behavior and wall clearance of the designed double-element airfoil are simulated and studied to find the optimum angle of attack for the two elements.

2. Theory

Reynolds' Average Navier-Stoke (RANS) is an idea first proposed by Reynolds [6]. It is a turbulence flow modeling method in which flow variables are decomposed into time-averaged and fluctuating components (Reynold decomposition). The basic concept of decomposition is to separate the flow variable (like velocity u) into the mean (time-averaged) component ($\bar{u}$) and the fluctuating component (u'). Therefore, the velocity can be written as

$$u(x,t) = \bar{u}(x,t) + u'(x,t)$$

where x = (x,y,z). Using these properties, the Navier–Stokes equations can be expressed in

$$\rho\left(\frac{\partial \bar{u}_i}{\partial t} + u'_k \frac{\partial \bar{u}_i}{\partial x_k}\right) = -\frac{\partial \bar{p}}{\partial x_i} + \frac{\partial}{\partial x_j}\left(\mu \frac{\partial \bar{u}_i}{\partial x_j}\right) + \frac{\partial R_{ij}}{\partial x_j} \quad (1)$$

The equation yields a nonlinear Reynolds stress term $R_{ij} = -\rho\overline{u'_i u'_j}$ that requires the additional model to fully resolve the problem. Turbulent model is the additional model to solve the Reynold stress term. Numerous turbulence models for RANS computing have been developed. The most commonly used models are the k-ω group models.

k-ω group model was proposed by Wilcox [7] in 1998. It is a very popular model group because the governing equation does not contain the non-calculating term on the wall. As a result, the calculation can be integrated from the wall without using the wall function. The models in this family are highly accurate. and robust for near-wall flow with a pressure gradient.

2.1 Standard k-ω (SK-ω) Model

Standard k-ω (SK-ω) model is widely used in aerodynamics and turbine machinery. Additional sub-models were applied to accommodate the compressible effect. including adjustment of transition flow and shear flow. For the standard k-ω model, the variables k and ω can be calculated from the following equation:

$$\frac{\partial}{\partial t}(\rho k) + \frac{\partial}{\partial x_i}(\rho k u_i) = \frac{\partial}{\partial x_j}\left(\Gamma_k \frac{\partial \mathrm{k}}{\partial x_j}\right) + G_k + Y_k + S_k \quad (2)$$

$$\frac{\partial}{\partial t}(\rho \omega) + \frac{\partial}{\partial x_i}(\rho \omega u_i) = \frac{\partial}{\partial x_j}\left(\Gamma_\omega \frac{\partial \mathrm{k}}{\partial x_j}\right) + G_\omega + Y_\omega + S_\omega \quad (3)$$

where G_k represents the turbulent kinetic energy (k) generated by the mean velocity gradient. where G_ω is ω being generated, while Γ_k and Γ_ω represent the effective diffusivity of k and ω, respectively. Y_k and Y_ω are the dissipation rates of k and ω, respectively, while S_k andS_ω are the source terms that can be defined.

Standard k-ω has superior performance for wall-bounded boundary layer, free shear, and low Reynolds number flows compared to models from the k-ε family. It is suitable for complex boundary layer flows under adverse pressure gradients and separation (external aerodynamics and turbomachinery). Separation can be predicted to be excessive and early. However, it is inaccurate for adverse pressure gradients, strong curvature, and jet flow. Moreover, it is oversensitive to inlet free-stream turbulence properties and sensitive to an initial guess.

2.2 Shear Stress Transport k-ω (SST k-ω) Model [8]

It is a model that uses a blending function to gradually change from the standard k-ω model at the boundary layer. to the k-ε model for the version for high Reynolds numbers in the inviscid region. The model includes modifications to turbulent viscosity to explain the transfer effect of principal turbulent shear stress.

$$\frac{\partial}{\partial t}(\rho k) + \frac{\partial}{\partial x_i}(\rho k u_i) = \frac{\partial}{\partial x_j}\left(\Gamma_k \frac{\partial \mathrm{k}}{\partial x_j}\right) + \tilde{G}_k - Y_k + S_k \tag{4}$$

$$\frac{\partial}{\partial t}(\rho \omega) + \frac{\partial}{\partial x_i}(\rho \omega u_i) = \frac{\partial}{\partial x_j}\left(\Gamma_\omega \frac{\partial \mathrm{k}}{\partial x_j}\right) + G_\omega - Y_\omega + D_\omega + S_\omega \tag{5}$$

where $\tilde{G}_k$ represents the turbulent kinetic energy (k) created due to the mean velocity gradient.

The SST k-ω offers similar benefits as standard k –ω. It is not overly sensitive to inlet boundary conditions like the standard k –ω, while provides more accurate prediction of flow separation than other RANS models. It overestimates turbulence in regions with high normal strain (but better than k-ε however) and converges slowly. It is better to use the other model for initial guess

2.3 Transition Shear Stress Transport k-ω (Transition SST K-ω)

It is a model that combines the governing equation of the SST k- ω model with the other two equations. The first equation is the equation for intermittency, γ, and the other equation is Transition onset criteria, which takes the form of the Momentum-thickness Reynolds number. The two equations added here were developed by Langtry and Menter [9] to cover the bypass transition and low free-stream turbulence, The Transition SST model is therefore able to predict the transition flow better than the SST model. The added intermittency equation is as follows.

$$\frac{\partial}{\partial t}(\rho \gamma) + \frac{\partial}{\partial x_i}\left(\rho \gamma U_j\right) = P_{\gamma 1} - E_{\gamma 1} + P_{\gamma 2} - E_{\gamma 2} + \frac{\partial}{\partial x_j}\left[\left(\mu + \frac{\mu_t}{\sigma_\gamma}\right)\frac{\partial \gamma}{\partial x_j}\right] \tag{6}$$

where $P_{\gamma 1}$ $E_{\gamma 1}$ are the transition source and $P_{\gamma 2}$ and $E_{\gamma 2}$ are destruction/re-laminarization source. The equation for calculating transition momentum thickness Reynolds number is $\widetilde{Re}_{\theta t}$

$$\frac{\partial}{\partial t}\left(\rho \widetilde{Re}_{\theta t}\right) + \frac{\partial}{\partial x_i}\left(\rho U_j \widetilde{Re}_{\theta t}\right) = P_{\theta t} + \frac{\partial}{\partial x_j}\left[\sigma_{\theta t}(\mu + \mu_t)\frac{\partial \widetilde{Re}_{\theta t}}{\partial x_j}\right] \tag{7}$$

This model is also sometimes known as the "gamma-Retheta-SST" model

2.4 Near-Wall Turbulence

The turbulence in the near-wall layer can be broadly divided into three layers. The innermost layer is called the viscous sublayer. In this part, the flow is almost a laminar flow. Viscosity plays an important role in the transfer of momentum as well as mass and heat. The part of the outermost layer is called the fully turbulence layer, in which turbulence plays the most important role. And finally, is the middle layer between the outer and inner layers called the buffer layer or blending region. This layer is affected by both viscosity and turbulence to a similar degree. To

calculate the viscosity effect on the viscous sub-layer, the grid in the viscous sublayer region is required to be small enough to be able to perform calculations in that area. The y+ values of each layer are as follows, the viscous sublayer y+<5, buffer layer or blending region 5 < y+ < 30, fully turbulent or log-law layer y+ > 30 to 60 [10]. In the case of the detailed calculations in the viscosity sublayer and buffer layer, the centroid of the first grid must be set at $y^+ \approx 1$. Before generating the grid. y+ can be pre-determined from the following equation.

$$y^+ = \frac{yu_\tau}{\nu} \tag{8}$$

where, u_τ is the so called friction velocity, y is the absolute distance from the wall and ν is the kinematic viscosity

3. CFD Model

This research is divided into two steps: the first begins with a simulation of the flow of a single airfoil first to validate the simulation compared with the data from literature [11]. The most accurate turbulence model was then compared. Once the separation onset was obtained, the data was used to design the double element airfoil. In Step 2, a flow through the double element air foil was simulated using the most accurate turbulent model from Step 1. The simulation will be performed to study the aerodynamic behavior, find the optimum angle of attack to enhance the maximum downforce, and finally, study the effects of ground clearance.

To select the airfoil section, the Reynolds number was first calculated with an upwind velocity of 120 km/h and a chord length of 0.6 m. By calculation, the Reynolds number is approximately 1.2×10^6 which is in the turbulent regime. However, if the air foil was split into 2 pieces, the chord length would be reduced to only 0.2-0.4 meters so that it could be installed in a limited space, resulting in the Reynolds number being in the range, about 3×10^5 to 5×10^5 which considers that the flow is in the low Reynolds regime (Re in the range from 6×10^4 to 5×10^5) The S1223 is an airfoil that was designed for use in the low Reynolds number range and offers high lift characteristics. Therefore, this article selects S1223 as the air foil to design the double-element air foil. Figure 1 shows the profile geometry and size of S1223 airfoil designed based on the Reynolds number mentioned above.

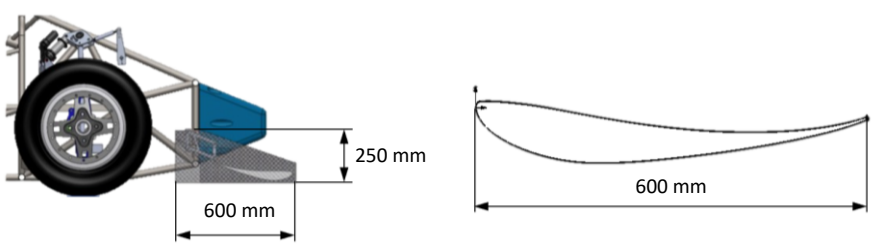

Fig. 1. S1223 airfoil profile.

On the assumption that the front wing attaches to the end plate to prevent tip loss at the wing tips, so, it can be deduced that the flow is two-dimensional. The two-dimensional domain was constructed using SolidWork software. The airfoil has a chord length of 0.6 m. The domain characteristics are shown in Fig. 2.

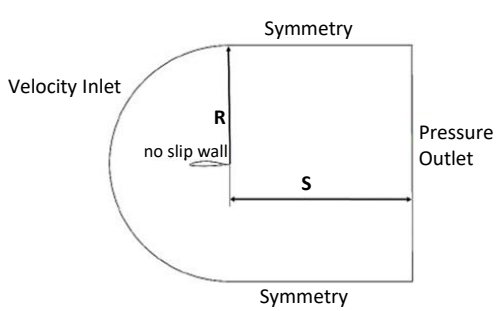

Fig. 2. Domain and Boundary

where R = *50* times the chord length and S = *60* times the chord length, the boundary conditions at the entrance were velocity inlet, on the top and the bottom was symmetry, at the exit was pressure outlet, and no slip wall condition on the wall surface of the airfoil. Because the flow around the airfoil is primarily affected by the viscous on the wall surface. Calculating the flow around the airfoil must consider the boundary layer flow. The key principle is to control the size of the grid near the wall surface to be smaller than the boundary layer thickness. That is to say, there must be at least 10 grids under the boundary layer thickness. Therefore, in this place, the centroid of the first grid was placed at y+< 10. The grid surrounding the airfoil was an inflation quadrilateral mesh which gradually grew with a growth rate of 1.12. The outer inviscid region mesh was set by using a triangle grid. The grid generated using Ansys Meshing is shown in Fig. 3.

.

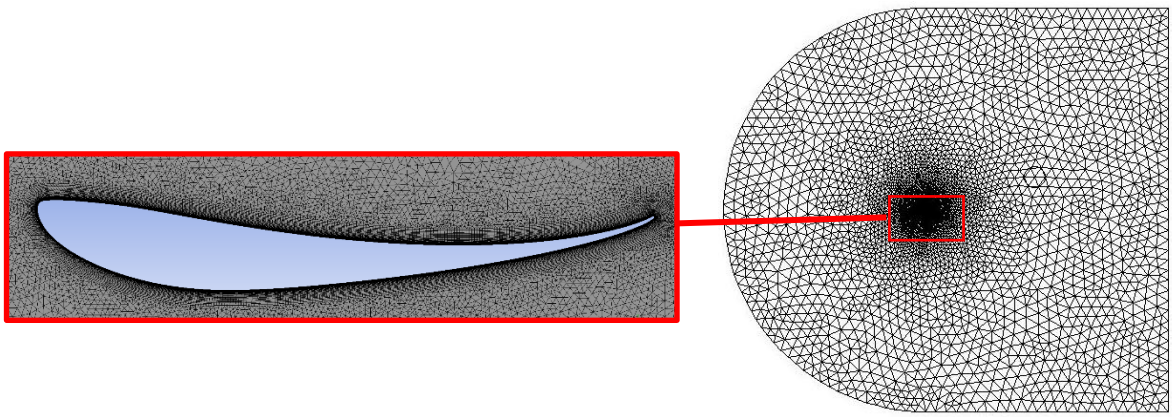

Fig. 3. Grid in the hold domain and surrounding the airfoil.

The assumption was that the flow was steady and 2 dimensional (no tip losses). The calculation is running on Fluent©. The solver used in the calculation was pressure-based, with the SIMPLE pressure-velocity coupling scheme. The spatial discretization was "least squares cell based" for gradient, "second order" for pressure, and "second order upwind" for momentum, turbulence kinetic energy, and special discretization. The convergence absolute criteria for residuals of x, y, velocity, continuity, and kinetic energy is 10^{-8}. The simulation was run with a course grid at the beginning, then refined until the result was less than 10-8 changes.

4. Results and Discussions

From a single element airfoil simulation with three turbulence models compared, shown in Fig. 4, the simulation results indicated that the lift and drag coefficients obtained from the simulations correspond to the experimental values in the research literature [11].

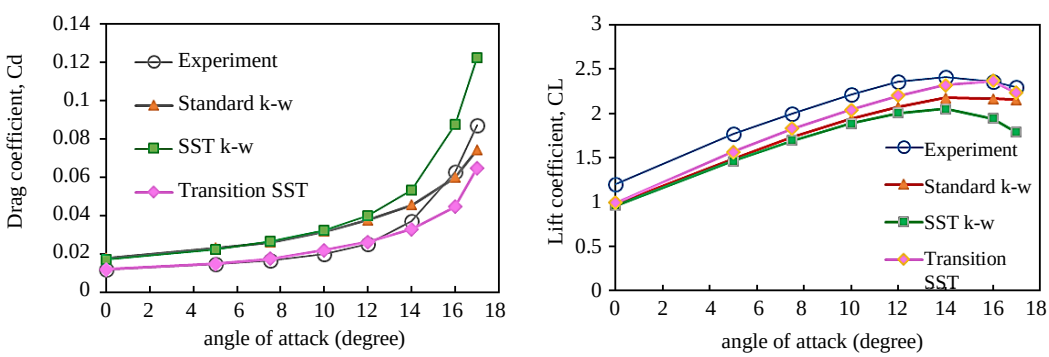

Fig. 4. Lift and drag coefficient & angle of attack compared to the experimental value [11].

By considering the lift coefficient, the stall occurs at an angle of approximately 14 degrees, which gives a maximum C_L of approximately 2.3 and C_d of approximately 0.3. For the lift coefficient, the most accurate turbulence model is the Transition SST k-ω model, which is the most accurate in both the pre-and post-stall regions. For the drag

coefficient, the most accurate model in the pre-stall period is the Transition SST k-ω model, with SST k-ω and standard k-ω being equally accurate. While in the post-stall region, the standard k-ω model was the most accurate, while the transition SST k-ω model gave under prediction and the SST k-ω model gave over prediction. The calculated wall shear stress on the airfoil surface is shown in Fig. 5. The graph shows that zero wall shear stress appears at a position of 0.4275 meters. on the suction side of the airfoil. This indicates the separation onset where the separation flow starts to occur. The streamline is shown in Fig. 6, the result indicates that a flow separates at 0.4275 m.

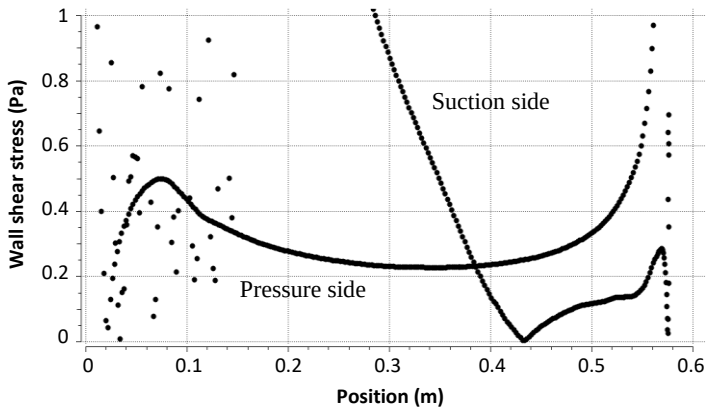

Fig. 5. Wall shear stress on the airfoil surface.

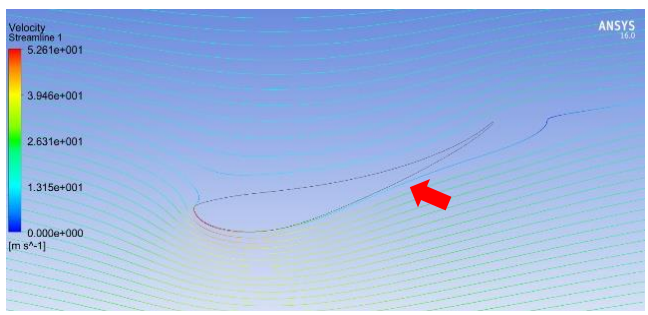

Fig. 6. Streamline around airfoil.

The separation onset position is used in the design of the double element airfoil to create a gap that causes the flow from the pressure side to interfere with the separation flow on the suction side, thereby causing the stall to be delayed and get higher C_L. The designed double element airfoil consists of the first element and second element airfoil placed next to each other with a gap as shown in Fig. 7.

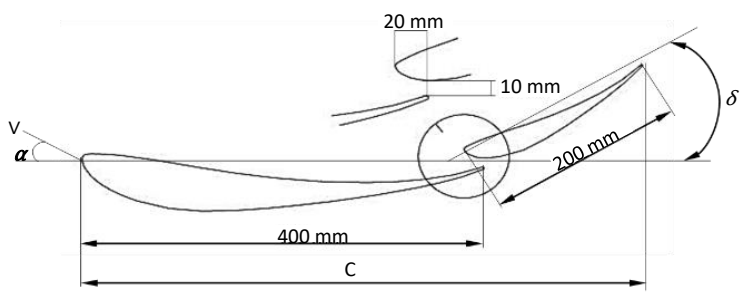

Fig. 7. Geometry of the designed double element airfoil

The gap is 2.5% of C (single element wing chord length) and the overlap is 5% of C. The simulation also includes the ground clearance study.

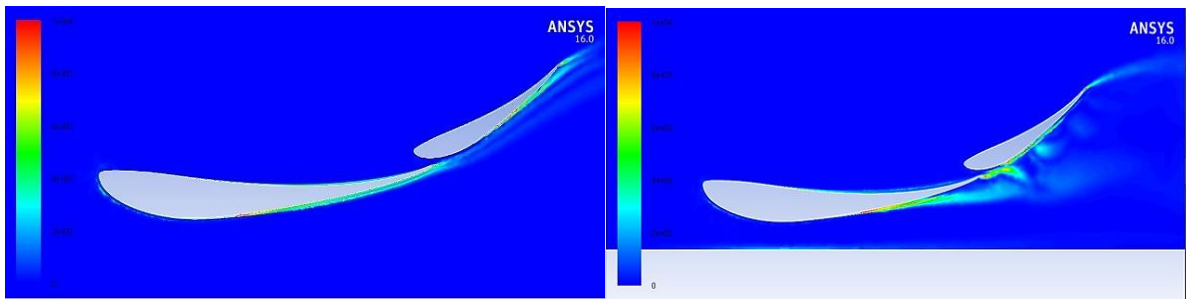

(a) (b)

Fig. 8. Vorticity contour (a) no ground clearance (b) with ground clearance.

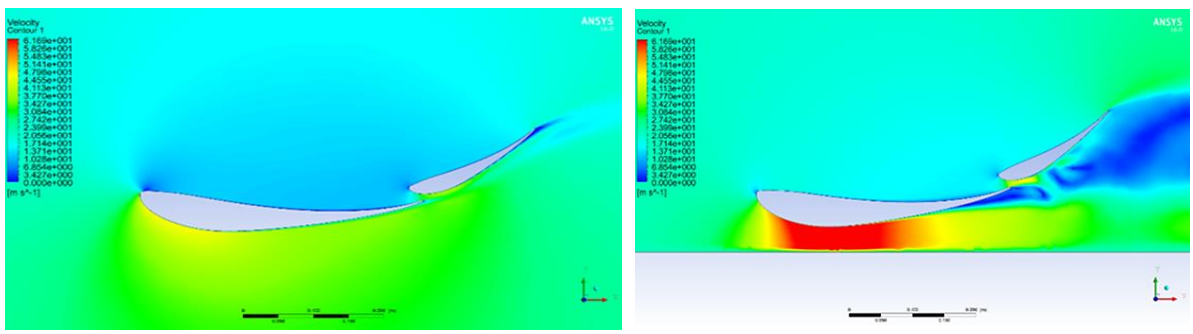

(a) (b)

Fig. 9. Velocity contour (a) no ground clearance (b) with ground clearance.

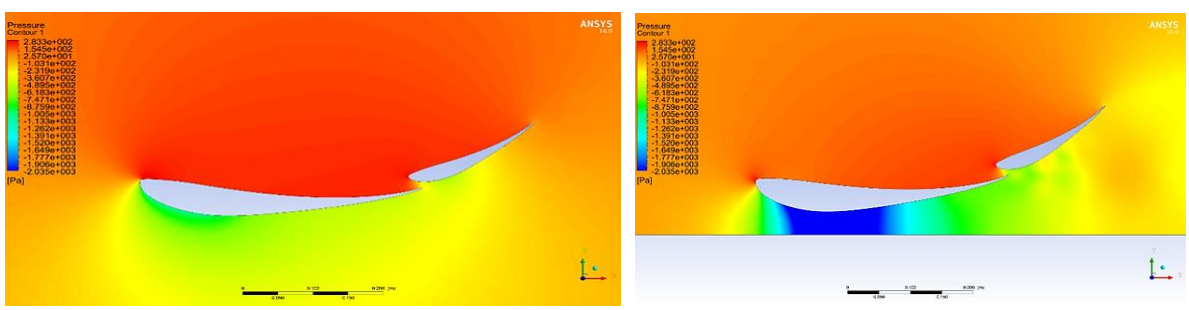

(a) (b)

Fig. 10. Pressure contour (a) no ground clearance (b) with ground clearance.

Figures 8 and 9 show the vorticity and velocity contours around the airfoil placed in space compared to the airfoil with the road surface below. The rear wake of the airfoil with the floor below has a wider wake area. This results in greater pressure differences in the front and back. Consequently, the drag force will increase as well. In addition, when considering Fig. 10, when there is a floor below, the pressure on the pressure side is higher than if there is no floor. This results in a greater pressure difference between the pressure side and the suction side, resulting in a higher downforce.

In numerical experiments to determine the optimum value of the angle of attack, the angle of attack of first element wings varied in the range of -6 to 17 degrees, and the second element airfoil ranged from 30 to 60 degrees. The results of the lift and drag force are shown in Fig. 11. From the graph, it can be seen that the angle of attack of the first element airfoil has a remarkable effect on downforce in the range of 3 to *3* degrees. It gives a higher downforce than

the other angles. The angle of attack that gives the maximum down force is 3 degrees, resulting in a maximum down force of 884.3 N with a CL value of 4.8737, Cd of 0.34655, and a drag force of 62.88 N. The effect of the angle of the second element wing. The tendency tends to decrease the downforce as the second element wing's angle increases. The angle of attack of the second element airfoil that yielded the maximum down force in the experiment was 30 degrees. It was found that there was a tendency to get a higher down force if the second element airfoil angle was reduced.

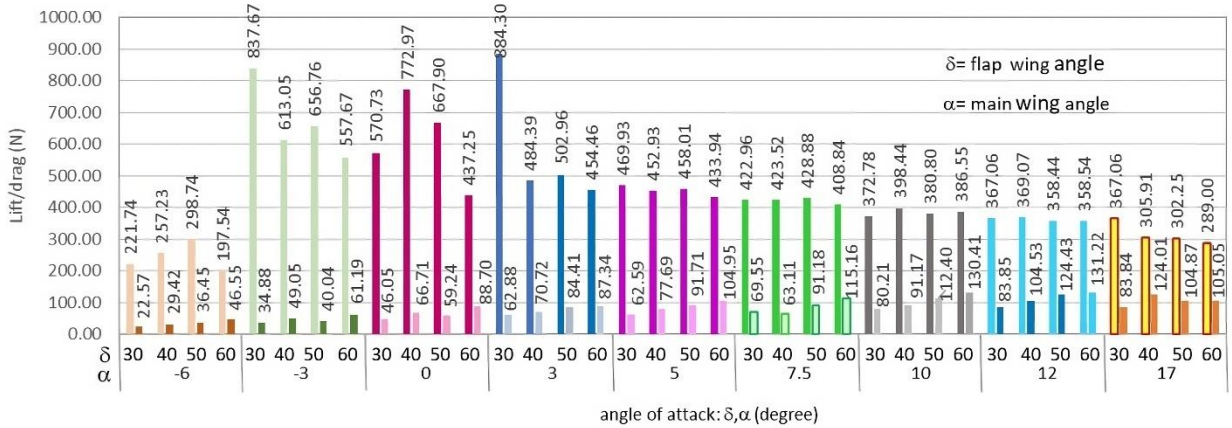

Fig. 11. Lift and drag force at the various angle of attack of the first and second element wing.

5. Conclusions

From the numerical experiment, the results of a single-element airfoil simulation using RANS agreed with the experimental values. Ground clearance had a significant impact on the calculated solution. The turbulence model with the highest accuracy is the Transition SST k-ω model. In conclusion, it can be concluded that RANS is a powerful and accurate method for solving turbulent flow. The method is extremely useful for the analysis and design of double-element airfoil. The designed double element airfoil provides better lift coefficients and downforce than the basic single element airfoil. An optimum angle of attack for both main and second-element wing wings can be found. However, in flow simulations, the effect of ground clearance must be considered to get the most accurate result. Finally, simulation methods used in this research can be applied to similar aerodynamic flow problems.

Nomenclature

$\bar{u}$	mean (time-averaged) velocity component, m/s
R_{ij}	Reynold stress, N/m^2
u'	fluctuating velocity component, m/s
ν	kinematic viscosity, m^2/s
$\tilde{G}_k$	turbulent kinetic energy (k) created due to the mean velocity gradient, J/kg
Γ_k	effective diffusivity of k, kg/m. s
Γ_ω	effective diffusivity of ω, kg/m. s
$E_{\gamma 1}$	transition source
$E_{\gamma 2}$	re-laminarization sources
G_k	turbulent kinetic energy (k) generated by the mean velocity gradient, J/kg
G_ω	ω being generated, 1/s
$P_{\gamma 1}$	transition source
$P_{\gamma 2}$	destruction sources
S_k	source terms, m^2/s^3
S_ω	source terms. m^2/s^3
Y_k	dissipation rates of k m^2/s^3
Y_ω	dissipation rates of ω, m^2/s^3

u velocity m/s
u_τ friction velocity, $s/^{m1/3}$
y absolute distance from the wall, m

References

[1] Seljak G. Race car aerodynamics. Slovenia: Department of physics, Faculty of mathematics and physics, University of Ljubljana; 2008.
[2] Katz J. Aerodynamics of race cars. Annu Rev Fluid Mech. 2006;38:27-63.
[3] Jasinski W, Selig M. Experimental study of open-wheel race-car front wings. SAE Tech Pap. 1998:2549-2557.
[4] Ranzenbach R, Barlow J, Diaz RH. Multi-element airfoil in ground effect-an experimental and computational study. 15th Applied Aerodynamics Conference; 1997 Jun 23-25; Atlanta, USA. USA: AIAA; 1997. p. 1-9.
[5] Zhang X, Zerihan J. Aerodynamics of a double-element wing in ground effect. AIAA J. 2003;41(6):1007-1016.
[6] Reynolds O. IV. On the dynamical theory of incompressible viscous fluids and the determination of the criterion. Philos Trans Royal Soc London A. 1895;186:123-164.
[7] Wilcox DC. Turbulence modeling for CFD, Vol. 2. La Canada: DCW industries; 1998.
[8] Menter FR. Review of the shear-stress transport turbulence model experience from an industrial perspective. Int J Comput Fluid Dyn. 2009;23(4):305-316.
[9] Langtry RB, Menter FR. Correlation-based transition modeling for unstructured parallelized computational fluid dynamics codes. AIAA J. 2009;47(12):2894-2906.
[10] ANSYS. Fluent 6.2 User's Guide. Canonsburg: ANSYS Inc; 2013.
[11] Selig MS, Guglielmo JJ. High-lift low Reynolds number airfoil design. J Aircr. 1997;34(1):72-79.